metals

Article

Damping Analysis of High Damping MgO/Mg Composites in Anelastic and Microplastic Deformation

Diqing Wan *, Fan Yang, Jiajun Hu, Shaoyun Dong, Hao Tang, Yu Wang, Yandan Xue, Guoliang Han, Jie Kang, Jingwen Xu and Guanmei Zeng

School of Materials Science and Engineering, East China Jiaotong University, Nanchang 330013, China
* Correspondence: divadwan@163.com; Tel.: +86-0791-87046102; Fax: +86-0791-87046122

Abstract: In this study, MgO/Mg composites were prepared using direct melt oxidation to verify the effects of elastic deformation and microplastic deformation on the damping properties. It was found that the composites have high damping properties at a certain strain amplitude, which indicated that the damping properties of the magnesium matrix were effectively enhanced by the in situ-synthesized oxide particle. In addition, other damping mechanisms different from the G–L dislocation damping mechanism exist in MgO/Mg composites, i.e., the damping mechanism of the microplastic deformation, leading to a model of microplastic deformation damping established and its mechanistic analysis.

Keywords: magnesium matrix composites; anelastic damping; microplasticity damping

check for updates

Citation: Wan, D.; Yang, F.; Hu, J.; Dong, S.; Tang, H.; Wang, Y.; Xue, Y.; Han, G.; Kang, J.; Xu, J.; et al. Damping Analysis of High Damping MgO/Mg Composites in Anelastic and Microplastic Deformation. *Metals* **2023**, *13*, 445. https://doi.org/10.3390/met13030445

Academic Editors: Xiaolong Ma and Tianhao Wang

Received: 16 December 2022
Revised: 28 January 2023
Accepted: 7 February 2023
Published: 21 February 2023

1. Introduction

With the rapid development of modern industry, various mechanical problems caused by vibration and noise have become increasingly serious, especially in many precision instruments [1]. Therefore, the development of excellent damping materials has been thrust into public view. Magnesium and its alloys have become the focus of attention in this research field [2]. Magnesium alloys have a wide range of industrial applications due to their low density, high specific strength, adequate mechanical properties and excellent damping properties [3–6]. As a new engineering material with excellent damping properties, most of the main research and development directions of magnesium-based damping materials are aimed toward retaining the advantages of their high specific strength while maximizing their damping properties [7,8]. So, in order to achieve this goal, it is a valuable research option to investigate how to enhance the damping properties of magnesium matrix composites. Srikanth [9] investigated the effect of nanoscale alumina particles of the damping ability of pure magnesium and found that the damping value of the composites increased by 34% compared to pure magnesium [10]. Several researchers have also continued their research for nanoscale magnesium oxide, including applications in nuclear technology-related fields [11–13], yet relatively little research has been carried out on the enhancement of pure magnesium by nanoscale magnesium oxide. Therefore, if MgO can be dispersed into the matrix, the damping properties of the material will be greatly improved, due to its principle of promoting damping ability by enhancing local stress and local plastic deformation around the particles. In this study, an attempt was made to prepare a new MgO/Mg matrix composite by directing melt oxidation method. The preparation method is particularly concise and economical because the magnesium oxide is formed by the in situ reaction to against molten magnesium and air, which reduces the addition of excess materials.

Although the main damping mechanism of magnesium alloys is known as the G–L dislocation damping mechanism, in fact, other microplastic damping mechanisms may occur to certain large strain amplitudes. Therefore, clarifying the role of the damping mechanism of magnesium alloy materials under microplastic deformation on the damping properties has a crucial impact on the development of new damping magnesium matrix composites [14]. Fan [15] investigated the microplastic deformation behavior of pure magnesium and magnesium alloys and judged that when microplastic deformation occurs in pure magnesium, the dislocations of the dependent grains simultaneously produce basal slip, and the damping properties of the material will be better [16,17]. However, the damping mechanisms present in the microplastic deformation of magnesium matrix composites have not been investigated more thoroughly because most of the current studies are related to the G–L dislocation damping theory of the material. This is mainly due to the difficulty of experimental techniques related to microplastic deformation and its complex influences, resulting in a relative lack of research on the microplastic theory of materials and the transition mechanisms from analysis to microplastic deformation. Thus, the other aim of this work provides new methodological and experimental guidance for the study of the damping properties of magnesium-based materials in analysis and microplastic damping.

2. Experimental

2.1. Preparation of Samples

In this study, pure commercial magnesium ingots (99.95% purity, from China Jiangxi Qunxin Strong Magnetic New Material Co, Ltd., Ganzhou, China) were used as the substrate material. The melting point of pure magnesium is about 648 °C, so the set oxidation temperature was 680 °C. The oxidized melt was mechanically stirred at 800 rpm for 2 min, and then the melt was poured into a metal mold for air cooling.

2.2. Characterization of Materials

Samples were polished, cleaned, and soaked in 3% nitric acid/alcohol for 5–8 s. The microstructure was observed using an optical microscope (OM, COOLPIX-4500). The interfacial morphology of the MgO/Mg composites was observed with a scanning electron microscope (SEM, GeminiSEM 500). To measure the damping capacity of 35 mm × 5 mm × 1 mm, rectangular bending beam specimens were cut with an EDM cutter. The damping capacity was measured using a Dynamic Mechanical Analyzer (DMA Q800) in a single cantilever vibration mode with a vibration frequency of 1 Hz. The specimens used for damping measurements were mounted on a DMA gripping head. The resulting sinusoidal force and deflection data were recorded and the damping capacity of the material was evaluated using the loss tangent (tan δ), which is calculated as

$$Q^{-1} = \tan\ \delta = \frac{E''}{E'} \tag{1}$$

where E'' is the loss modulus and E' is the storage modulus. The damping, with respect to strain amplitude, was tested at room temperature for strain amplitudes ranging from 1×10^{-4} to 4×10^{-3}.

3. Results and Discussion

3.1. Microstructure Analysis of MgO/Mg Composite

Figure 1 shows the microstructure of the composite prepared by oxidation of pure magnesium melt. It can be seen from the figure that the oxide particles are uniformly dispersed in the magnesium matrix, which indicates that the oxide particles produced by the oxidation of pure magnesium in the molten state were successfully stirred into the matrix by subsequent mechanical stirring. Thus, pure magnesium matrix composites reinforced by oxides were successfully prepared. The content of oxide particles increased with increasing oxidation time, and the oxide volume fraction was estimated by image analysis software to be about 1.7% for an oxidation time of 2 min.

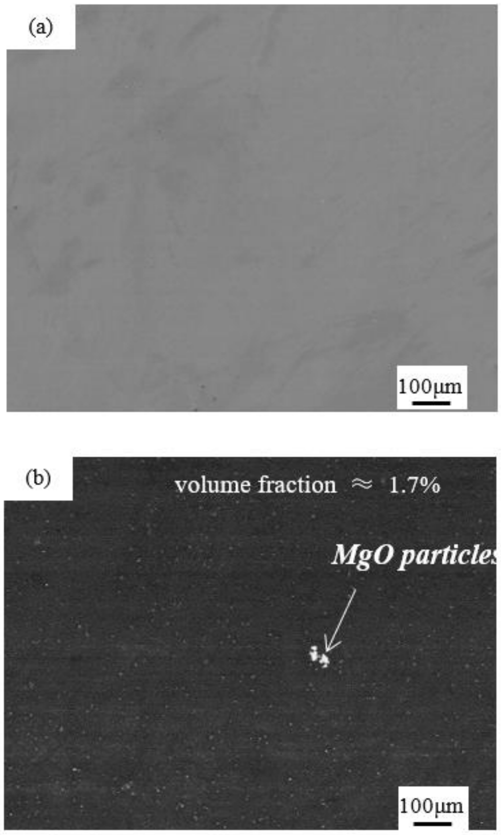

Figure 1. SEM micrographs of the MgO/Mg composites: (**a**) pure Mg; (**b**) oxidation for 2 min.

Figure 2 shows the XRD analysis pattern of the composites, from which it can be seen that the composites are mainly composed of MgO and Mg matrix, and the height of the MgO (200) diffraction peak increases significantly compared to the matrix due to the oxidation of the matrix material, which indicates the increase of its oxide content, which is significantly elevated compared to the normal melt–cast pure Mg matrix. Figure 3 shows the EDS spectrum of the MgO/Mg composite, from the figure it can be seen that the material contains a considerable amount of relatively uniformly dispersed carbon atoms, which is due to the fact that in the process of direct contact between the pure magnesium melt and air, the oxygen in it, CO_2 in the air can also react with magnesium at high temperature ($2Mg + CO_2 \rightarrow 2MgO + C$), and the reacted carbon atoms exist in the form of solute atoms in the matrix, forming weak pinners. In addition, due to the in situ reaction within the matrix, magnesium oxide particles (strong pinners) are produced. As a result, the number of both strong and weak pegs in the composite increases compared to pure magnesium, i.e., L_C and L_N decrease. On the other hand, according to G–L theory, the variation of dislocation density within the material has a direct effect on dislocation damping. It was found that the excessive difference in the coefficient of thermal expansion between the reinforcement and the matrix will lead to an increase in the dislocation density [18–20]. The residual strain can be initially estimated by the following equation [21].

$$\varepsilon = \Delta\alpha \cdot \Delta T \tag{2}$$

where $\Delta\alpha$ is the difference in the coefficient of thermal expansion between the matrix and the reinforcement, and ΔT is the difference in cooling temperature. In this study, the coefficient of thermal expansion of pure magnesium is about 26×10^{-6} °C^{-1}, the coefficient of thermal expansion of MgO is about 13×10^{-6} °C^{-1} [22], And the temperature difference during solidification of pure magnesium in the molten state is about 500 °C. The estimated residual strain ε is 0.6%, and the residual stress value near the interface between the matrix and the reinforced phase is about 0.6% × 45 GPa = 270 MPa. This value is much higher than the yield strength of cast pure magnesium (~25 MPa), and such a large internal stress is sufficient to cause the appearance of plastic strain zones and the generation of new dislocations. According to the prismatic model of dislocations, the dislocation density can be calculated by the following equation [23].

$$\rho = \frac{B\varepsilon V_p}{ba_i(1 - V_p)} \tag{3}$$

where ε is the mismatch strain resulting from the difference in thermal expansion coefficients between the matrix and the reinforcing phase, V_p is the volume fraction of the reinforcing phase, a_i is the minimum size of the reinforcing phase, and B is the geometric constant. The above equation shows that the density of dislocations is directly proportional to the volume fraction of the reinforcing phase and inversely proportional to the minimum size of the reinforcing phase. Therefore, the dislocation density of the composite increases with the increase of the volume fraction of the reinforcing phase.

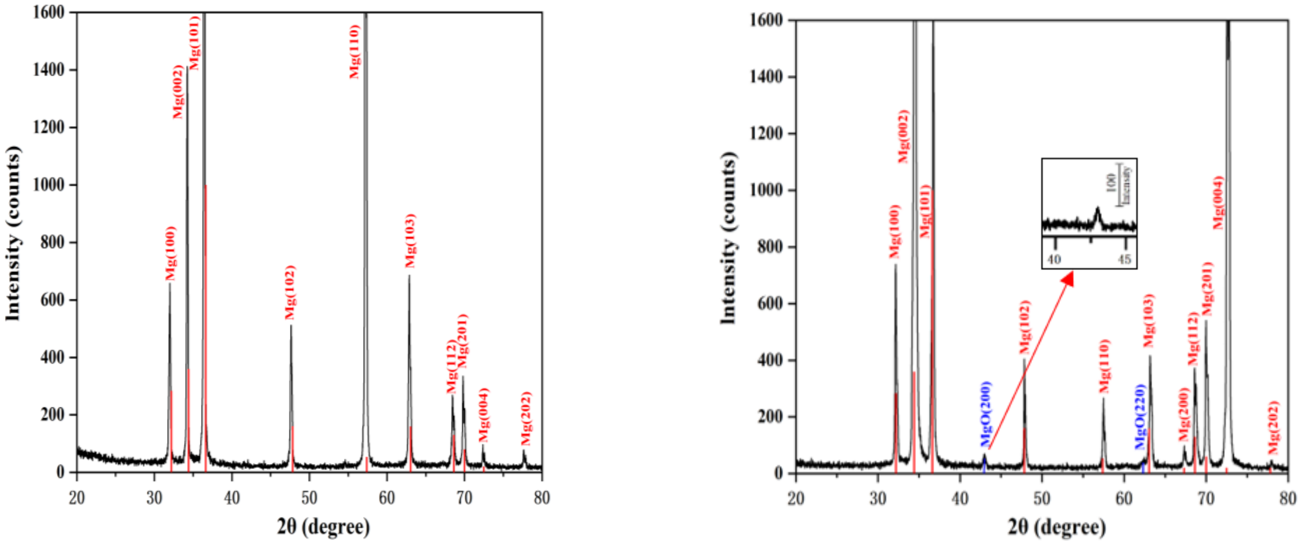

(**a**) (**b**)

Figure 2. XRD spectrum of pure Mg and in situ MgO/Mg composite (**a**) pure Mg; (**b**) oxidation for 2 min.

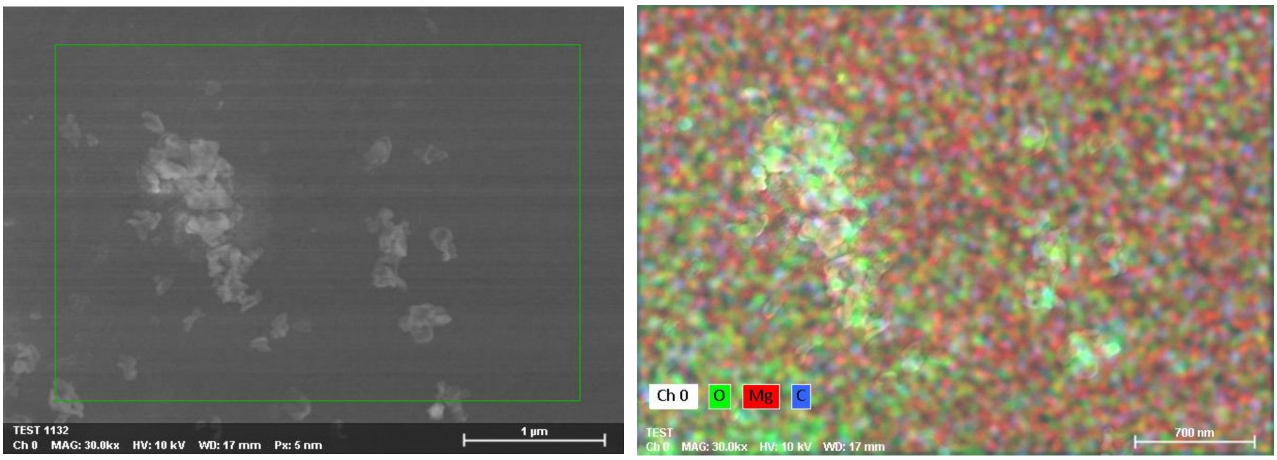

Figure 3. *Cont.*

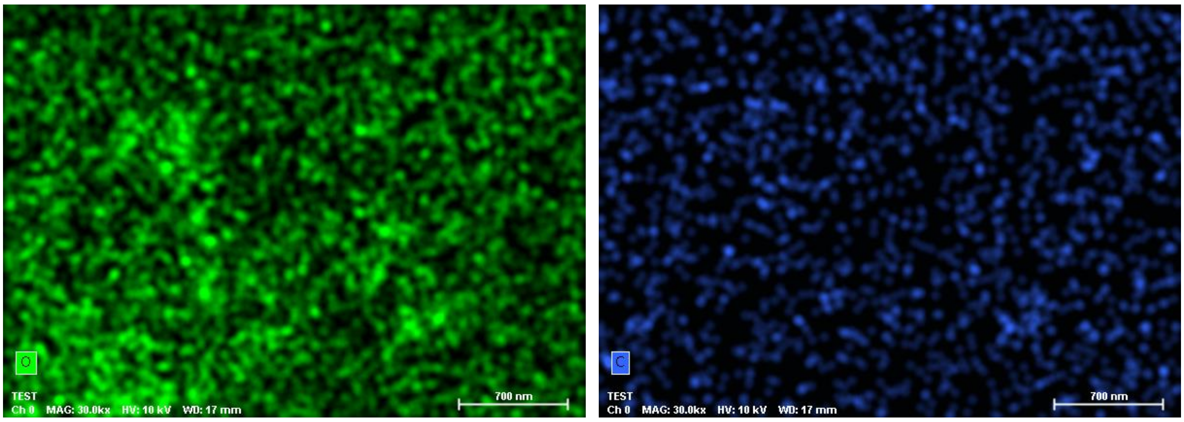

Figure 3. The EDS analysis results of the MgO/Mg composites.

3.2. Anelastic Damping of MgO/Mg Composites

Among the metallic structural materials, pure magnesium has the highest damping performance, and it is usually believed that its high damping performance is mainly attributed to the long and smooth dislocation lines within the material sweeping back and forth under the action of external forces, thus causing the loss of vibrational mechanical energy, which is a typical dislocation damping material. According to the classical dislocation damping model (G–L model) proposed by Granato and Lücke [24,25], in metallic materials, dislocation lines are pinned by strong pinners (dislocation nodes, secondary phase and grain boundaries) and weak pinners (impurity atoms, sites, etc.), and when the applied stress is not significant, the dislocation lines "bow out" at the weak pinners. When the applied stress is not large, the dislocation line "bows out" between the weak pinners, the dislocation string does reciprocal motion with periodic stress oscillation, due to the point defects in the crystal and the dislocation produces elastic interaction, thus causing energy loss; at this time, the dislocation swept area is small, the dislocation is less movable, resulting in strain–amplitude-independent damping, recorded as Q_0^{-1} . When the strain increases so that the dislocation line undergoes avalanche debonding (exceeding the critical strain amplitude value), and the debonding consumes energy at the same time. then the dislocation line oscillates with the stress oscillation between the strong nailing points, and sweeps through the weak nailing points, the movability of the dislocation increases, then with the increase in strain amplitude, the dislocation line oscillation area increases, the damping value increases rapidly, recorded as Q_h^{-1} . The damping value of the material is expressed as, i.e.,

$$Q^{-1} = Q_0^{-1} + Q_h^{-1} \tag{4}$$

Among them:

$$Q_0^{-1} = \frac{\rho B L_C^4 \omega}{36 G b^2} \tag{5}$$

$$Q_h^{-1} = \frac{C_1}{\varepsilon} \exp\left(-\frac{C_2}{\varepsilon}\right) \tag{6}$$

In the formula $C_1 = \frac{\rho F_B L_N^3}{6bEL_C^2}$; $C_2 = \frac{F_B}{bEL_C}$; B is a constant; is the density of movable dislocations; b is the Burgers vector of dislocations; ω is the angular frequency; G is the shear modulus; L_C is the adjacent weak nail point spacing; L_N is the spacing between adjacent strong nailing points; F_B is the force between point defects and dislocations, and the average value is taken because the force between various point defects and dislocations is different; E is the modulus of elasticity.

Figure 4 compares the damping properties of pure Mg and MgO/Mg composites as a function of strain amplitude, from which it can be seen that the damping properties of the composites is greatly improved. At low strain amplitude, the damping performance of the composite has good performance. In the MgO/Mg composite, the damping curves still exhibit more typical dislocation damping characteristics, i.e., they are divided into strain amplitude weakly dependent segments and strain amplitude strongly dependent segments. To explain the variation of dislocation damping behavior within the composites, the variation of the number of strong and weak pinners and their movable dislocation density in the composites is considered according to the G–L model. At low strain amplitude, the corresponding damping value is proportional to ρ as shown in Equation (3). The presence of carbon atoms leads to a decrease in the spacing between weak pinners in the composite, but the dislocation density increases significantly due to thermal mismatch, and the damping value of the composite is still slightly higher than that of pure Mg at low strain amplitude. Moreover, the damping performance of the specimen with an oxidation time of 2 min is good at low strain amplitude, which may be due to the small number of weak pinners in this specimen compared with the pure magnesium matrix material, while its dislocation density is higher than that of pure magnesium, resulting in better damping performance at low strain amplitude. In the high strain amplitude stage, the dislocation lines discarded the weak pinners and started to oscillate between the strong pinners. The damping performance of the composite at high strain amplitude increased with the increase of oxide content. Based on the above analysis, it can be concluded that the in situ-synthesized magnesium oxide particles is beneficial to enhancing the dislocation damping of the magnesium matrix. Furthermore, by transforming Equation (6), it can be obtained that.

$$\ln(Q_h^{-1} \cdot \varepsilon) = \ln C_1 - C_2/\varepsilon \quad (7)$$

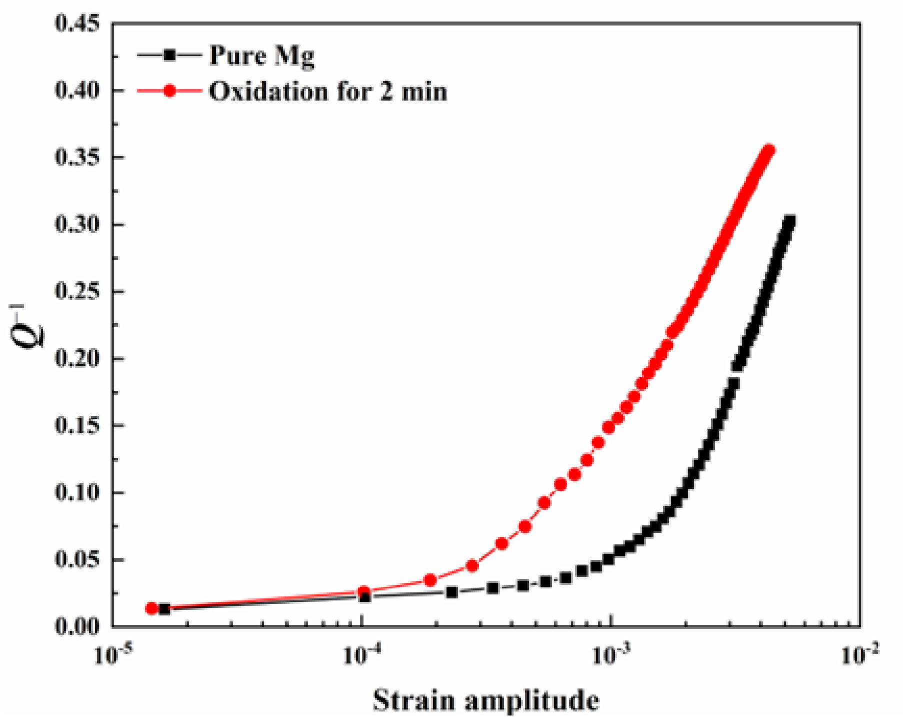

Figure 4. Strain amplitude-damping curve of MgO/Mg composites.

Therefore, the G–L curves of pure magnesium and composite materials can be plotted. The curve of the pure magnesium and composite in the εcr1 < ε < εcr2 interval can be approximated as a straight line, as shown in Figure 5b, which is in good agreement with the G–L dislocation damping theory. However, as shown in Figure 5a. the G–L plots deviate from this straight line at high stain amplitude, which indicates that there are other damping mechanisms in the composite. This leads to a higher damping performance of the composite material than the matrix material.

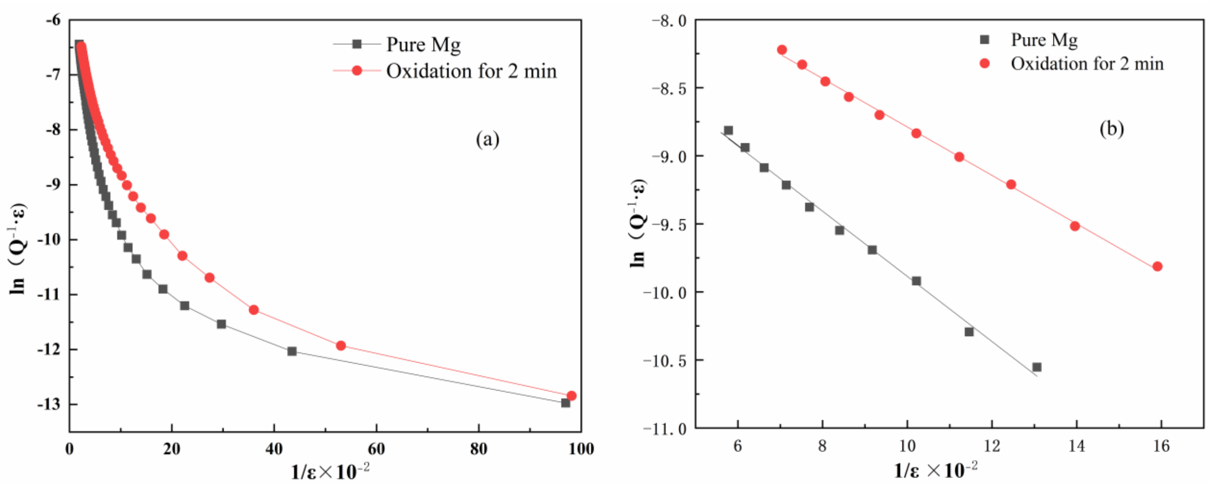

Figure 5. G–L curves of pure Mg and MgO/Mg composites: (**a**) the entire strain amplitude range; (**b**) εcr1 < ε < εcr2.

3.3. Microplastic Damping Mechanism of the Phase of MgO/Mg Composites

In the study of damping–strain amplitude correlation, Puškár A [26] divided the damping–strain amplitude curve of the material into four parts, as shown in Figure 6, with I and II being hysteretic elastic stages and III and IV being microplastic deformation stages.

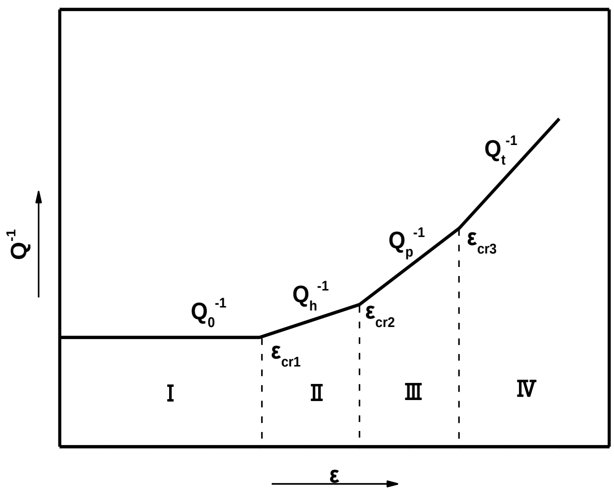

Figure 6. The relationship of damping and strain amplitude.

As referred above, the first critical strain amplitude (ε < εcr1) stage is the strain amplitude independent stage, according to the G–L model, the dislocation line is pinned by the weak pinners, and can only achieve reciprocal motion between the weak pinners, the damping value are weakly correlated to and strain amplitude. When the strain amplitude range is εcr1 < ε < εcr2, the dislocation line begins to rid itself of the weak pinners, to achieve reciprocal motion between the strong pinners. Dislocation mobility is greater than that of in stage I; hence, the strain amplitude dependent damping curves rise rapidly after εcr1. The dislocation structure of these two stages do not change, and the dislocation returns to the starting point after unloading, so the stages I and II are called hysteresis damping stages. This can be explained by the G–L model.

The damping related to the microplastic range in magnesium alloy is also a dislocation mechanism due to the movement of the dislocations. At the initial stage of microplastic deformation damping, the strain amplitude is εcr2 < ε < εcr3 and the dislocations are unpinned from the strong pinners and the dislocations slip on the base plan. When the strain amplitude is greater than εcr3, the dislocation slips on the base surface, gradually becoming entangled [27,28]. Peguin [29,30] first proposed a model to explain the damping phenomenon related to microplastic deformation. The microplastic-related damping can be expressed as follows:

$$Q_p^{-1} = \frac{A}{\pi \varepsilon h} \exp(B\varepsilon - B\varepsilon_p) \tag{8}$$

$$A = \frac{2\rho b v}{\pi f} \exp(-\frac{Q}{KT}) \tag{9}$$

$$B = \alpha \frac{VG}{KT} \tag{10}$$

where h is a constant, ε_p is the strain amplitude at the beginning of the microplastic deformation damping stage, ρ is the dislocation density, v is the intrinsic frequency of the dislocation, f is the test frequency, Q is the activation energy, α is the orientation factor, and G is the elastic shear modulus, and V is the dislocation activation volume. According to Equation (8), Equation (9) can be obtained:

$$\ln Q_p^{-1} \varepsilon = B\varepsilon + C \tag{11}$$

The $\ln Q_p^{-1} \varepsilon$ and ε curves are fitted to obtain a slope, B for calculating the slip.

It can be seen from Figure 7a that the damping value of the composite is higher than that of pure magnesium during the microplastic deformation stage. There are three main types of microplastic damping mechanisms in MgO/Mg composites: The first is dislocation damping mechanism. Fitting the curves to a straight line to approximate the activation volume of dislocations in the composite and pure Mg. It can be seen from Table 1 that the B value of the composite material is significantly larger than that of the matrix material. According to Equation (10), the B value is proportional to the activation volume of dislocations, so the dislocation activation volume of the composite material is larger than that of pure magnesium, so the damping of the composite material is better than pure magnesium. The second is phase interface damping mechanism. There is MgO particle reinforced phase in the composite material, and a good phase interface is formed between MgO and the magnesium matrix. Under the action of the strain amplitude, the phase interface moves and generates internal friction, which promotes improved damping performance. The third is a grain interface damping mechanism. In MgO/Mg composites, due to the addition of oxides, the grains are refined, and more grain boundaries increase to generate grain boundary damping. Therefore, under the action of various damping mechanisms, the damping value of the composite material is better than that of pure magnesium.

4. Conclusions

(1) In this study, a new biphasic magnesium oxide/magnesium composite was prepared using in situ oxidation. The damping properties of the in situ-oxidized MgO/Mg composite were greatly improved compared to pure magnesium.

(2) In the anelastic damping of the composites, the dislocation lines rid themselves of weak pinners and start to oscillate between strong pinners. The damping performance of the composites increases with the increase in strain amplitude. The in situ-synthesized oxide particle effectively enhances the damping capacity of the magnesium matrix.

(3) In the microplastic deformation of the composite, there are other damping mechanisms inside the composite that are different from the dislocation damping mechanism. The increase in the number of interfaces causes an increase in the interfacial damping contribution, which enhances the damping properties of MgO/Mg composites at high strain amplitudes.

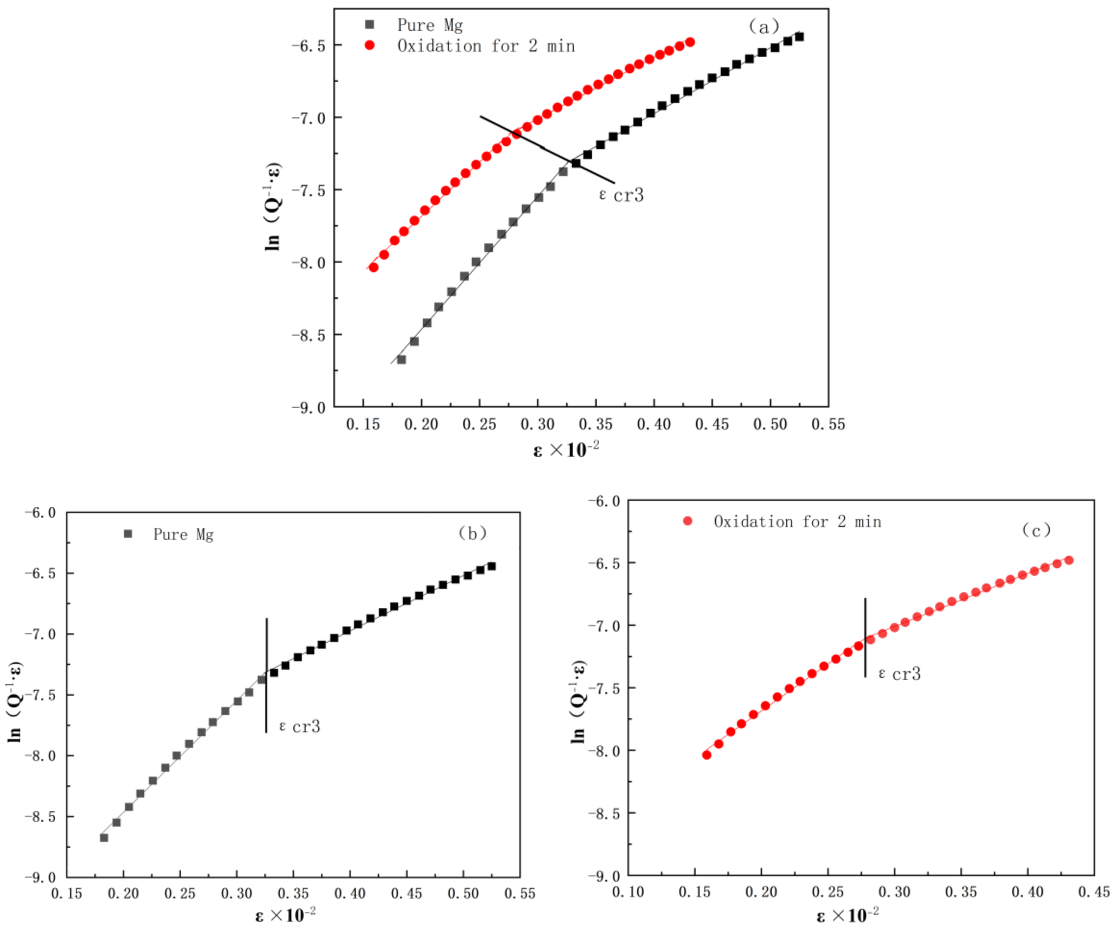

Figure 7. MgO/Mg composites material microplasticity curves: (**a**) all materials; (**b**) pure Mg; (**c**) oxidation for 2 min.

Table 1. Critical strain and B value of MgO/Mg composites.

Various Values / Material Type	$B_1 \cdot 10^2$	$B_2 \cdot 10^2$	$\varepsilon cr3 \cdot 10^{-2}$
Pure Mg	7.5272	4.2431	0.2875
Oxidation for 2 min	9.1827	4.5476	0.3020

Author Contributions: Conceptualization, D.W. and F.Y.; data curation, J.H., S.D., H.T., Y.W., Y.X., G.H., J.K., J.X. and G.Z.; writing—review and editing, D.W. and F.Y.; funding acquisition, D.W. All authors have read and agreed to the published version of the manuscript.

Funding: This work was supported by the National Natural Science Foundation of China (grant number 51665012); the Jiangxi province Science Foundation for Outstanding Scholarship (grant number 20171BCB23061, 2018ACB21020); and the Primary Research and Development Plan of Jiang Xi Province (grant number 2019BBEL50019).

Data Availability Statement: The datasets generated and/or analysed during the current study are not publicly available due [REASON WHY DATA ARE NOT PUBLIC] but are available from the corresponding author on reasonable request.

Conflicts of Interest: The authors declare no conflict of interest.

References

1. Zhang, Z.; Guo, Y.; Zhao, Y.; Chen, G.; Wu, J.; Liu, M. Effect of reinforcement spatial distribution on mechanical properties of MgO/ZK60 nanocomposites by powder metallurgy. *Mater. Charact.* **2019**, *150*, 229–235. [CrossRef]
2. Wang, X.; Wu, W.; Tang, Y.; Zeng, X.; Yao, S. Early high temperature oxidation behaviors of Mg-10Gd-3Y alloys. *J. Alloys Compd.* **2009**, *474*, 499–504. [CrossRef]
3. Song, J.; She, J.; Chen, D.; Pan, F. Latest research advances on magnesium and magnesium alloys worldwide. *J. Magnes. Alloys* **2020**, *8*, 1–41. [CrossRef]
4. Hu, X.; Zhang, Y.; Zheng, M.; Wu, K. A study of damping capacities in pure Mg and Mg-Ni alloys. *Scr. Mater.* **2005**, *52*, 1141–1145. [CrossRef]
5. Ramalingam, V.V.; Ramasamy, P.; Das Kovukkal, M.; Myilsamy, G. Research and Development in Magnesium Alloys for Industrial and Biomedical Applications: A Review. *Met. Mater. Int.* **2020**, *26*, 409–430. [CrossRef]
6. Wan, D.; Dong, S.; Hu, Y.; Hu, J.; Xue, Y.; Han, G. Strain Amplitude Dependence of High Damping Gr_p/Mg97Zn1Y2 Composites Ranging from Anelastic to Microplastic. *Metals* **2021**, *11*, 1570. [CrossRef]
7. Lin, L.; Liu, Z.; Chen, L.; Liu, T.; Wu, S. Microstructure evolution and low temperature superplasticity of ZK40 magnesium alloy subjected to ECAP. *Met. Mater. Int.* **2004**, *10*, 501–506. [CrossRef]
8. Huang, Z.; Qi, C.; Yang, G.; Lai, H.; Zhu, Y.; Zhi, C. Effect of Stress State in Rolling Deformation Zone of AZ31 Magnesium Alloy Plate on Edge Cracking. *J. Mater. Eng. Perform.* **2020**, *29*, 3906–3912. [CrossRef]
9. Srikanth, N.; Zhong, X.; Gupta, M. Enhancing damping of pure magnesium using nano-size alumina particulates. *Mater. Lett.* **2005**, *59*, 3851–3855. [CrossRef]
10. Popov, A.; Shirmane, L.; Pankratov, V.; Lushchik, A.; Kotlov, A.; Serga, V.; Kulikova, L.; Chikvaidze, G.; Zimmermann, J. Comparative study of the luminescence properties of macro- and nanocrystalline MgO using synchrotron radiation. *Nucl. Instrum. Methods Phys. Res. Sect. B Beam Interact. Mater. At.* **2013**, *310*, 23–26. [CrossRef]
11. Nikiforov, S.; Kortov, V.; Petrov, M. Luminescent and dosimetric properties of ultrafine magnesium oxide ceramics after high dose irradiation. *Radiat. Meas.* **2016**, *90*, 252–256. [CrossRef]
12. Baubekova, G.; Akilbekov, A.; Feldbach, E.; Grants, R.; Manika, I.; Popov, A.; Schwartz, K.; Vasil'Chenko, E.; Zdorovets, M.; Lushchik, A. Accumulation of radiation defects and modification of micromechanical properties under MgO crystal irradiation with swift 132Xe ions. *Nucl. Instrum. Methods Phys. Res. Sect. B Beam Interact. Mater. At.* **2020**, *463*, 50–54. [CrossRef]
13. Cui, Y.; Li, Y.; Sun, S.; Bian, H.; Huang, H.; Wang, Z.; Koizumi, Y.; Chiba, A. Enhanced damping capacity of magnesium alloys by tensile twin boundaries. *Scr. Mater.* **2015**, *101*, 8–11. [CrossRef]
14. Wu, Z.; Wang, J.; Wang, H.; Ma, S.; Huang, S.; Li, S.; Pan, F. Enhanced damping capacities of Mg–Ce alloy by the special microstructure with parallel second phase. *J. Mater. Sci. Technol.* **2017**, *33*, 941–946. [CrossRef]
15. Fan, G.; Zheng, M.; Hu, X.; Wu, K.; Gan, W.; Brokmeier, H.G. *Materials Science and Engineering: A*; John Wiley & Sons: Hoboken, NJ, USA, 2013; Volume 561, pp. 100–108. ISSN 0921-5093. [CrossRef]
16. Wang, C.-J.; Deng, K.-K.; Liang, W. High temperature damping behavior controlled by submicron SiCp in bimodal size particle reinforced magnesium matrix composite. *Mater. Sci. Eng. A* **2016**, *668*, 55–58. [CrossRef]
17. Malakar, C.; Trishul, M. Experimentation and optimisation of wear parameters of glass fibre-graphite reinforced composite. *Mater. Today* **2020**, *27*, 1431–1434. [CrossRef]
18. Wan, D.; Hu, J.; Wang, H.; Hu, Y.; Li, L. Ultra-High Damping Capacity of Oxide Reinforced Magnesium Matrix Composites by In Situ Synthesis. *Met. Mater. Int.* **2021**, *27*, 5399–5406. [CrossRef]
19. Hu, Y.; Deng, J.; Pan, F.; Zhang, D.; Chen, Y.; Wang, J. Study on damping capacity of graphite particle—Reinforced AZ31 magnesium matrix composites. *J. Compos. Mater.* **2020**, *45*, 557–564. [CrossRef]
20. Ghanbari, A.; Jafari, H.; Ghasemi, F.A. Wear Behavior of Biodegradable Mg-5Zn-1Y-(0-1)Ca Magnesium Alloy in Simulated Body Fluid. *Met. Mater. Int.* **2020**, *26*, 395–407. [CrossRef]
21. Wu, Y.; Wu, K.; Deng, K.-K.; Nie, K.B.; Wang, X.; Zheng, M.; Hu, X. Damping capacities and microstructures of magnesium matrix composites reinforced by graphite particles. *Mater. Des.* **2010**, *31*, 4862–4865. [CrossRef]
22. Wu, Y.; Wu, K.; Deng, K.-K.; Nie, K.B.; Wang, X.; Hu, X.; Zheng, M. Damping capacities and tensile properties of magnesium matrix composites reinforced by graphite particles. *Mater. Sci. Eng. A* **2010**, *527*, 6816–6821. [CrossRef]
23. Madeira, S.; Carvalho, O.; Carneiro, V.; Soares, D.; Silva, F.; Miranda, G. Damping capacity and dynamic modulus of hot pressed AlSi composites reinforced with different SiC particle sized. *Compos. Part B Eng.* **2016**, *90*, 399–405. [CrossRef]
24. Granato, A.; Lücke, K. Theory of Mechanical Damping Due to Dislocations. *J. Appl. Phys.* **1956**, *27*, 583–593. [CrossRef]
25. Granato, A.V.; Lucke, K. Application of Dislocation Theory to Internal Friction Phenomena at High Frequencies. *J. Appl. Phys.* **1956**, *27*, 789–805. [CrossRef]
26. Puškár, A. *Internal Friction of Materials*; Cambridge International Science Publishing: Cambrigde, UK, 2001; pp. 234–324. ISBN 9781898326502.
27. Yu, L.; Yan, H.; Chen, J.; Xia, W.; Su, B.; Song, M. Effects of solid solution elements on damping capacities of binary magnesium alloys. *Mater. Sci. Eng. A* **2020**, *772*, 138707. [CrossRef]
28. Wan, D.; Hu, J.; Hu, Y.; Wang, H. Anelastic and Microplastic Damping of an Mg-Zn-Y-Al Alloy. *Met. Mater. Int.* **2020**, *26*, 69–74. [CrossRef]

29. Peguin, P.; Perez, J.; Gobin, P. Amplitude-dependent part of the internal friction of aluminum. *Trans. Metall. Soc. AIME* **1967**, *239*, 438–450.
30. Wang, H.; Wang, H.; Zhang, R.; Liu, R.; Xu, Y.; Tang, R. Effect of high strain amplitude and pre-deformation on damping property of Fe-Mn alloy. *J. Alloys Compd.* **2019**, *770*, 252–256. [CrossRef]